J Forensic Sci, March 2006, Vol. 51, No. 2
doi:10.1111/j.1556-4029.2006.00060.x
Available online at: www.blackwell-synergy.com

Carme Rissech,[1,2] Ph.D.; George F. Estabrook,[3] Ph.D.; Eugenia Cunha,[1] Ph.D.; and Assumpció Malgosa,[2] Ph.D.

Using the Acetabulum to Estimate Age at Death of Adult Males*

ABSTRACT: The acetabular region is often present and adequately preserved in adult human skeletal remains. Close morphological examination of the 242 left male os coxae from the identified collection of Coimbra (Portugal) has enabled the recognition of seven variables that can be used to estimate age at death. This paper describes these variables and argues their appropriateness by analyzing the correlation between these criteria and the age, the intra- and interobserver consistence, and the accuracy in age prediction using Bayesian inference to estimate age of identified specimens. Results show significant close correlation between the acetabular criteria and age, nonsignificant differences in intra- and interobserver test, and 89% accuracy in Bayes prediction. Obtained estimated age of the specimens had similar accuracy in all ages. These results indicate that these seven variables, based on the acetabular area, are potentially useful to estimate age at death for adult specimens.

KEYWORDS: forensic science, forensic anthropology, human identification, human aging process, bone indicators, morphological details, Bayesian inference

The estimation of the age at death of adult human osteological remains is important for both Anthropology and Forensic Medicine. It is one of the more difficult tasks undertaken in these fields and it has remained a problem to be solved in anthropology and forensic medicine (1–5). Among present methods ((6–11) among others), those based on the os coxa take into account morphological modifications of the pubic symphysis (12–14) and the auricular surface (9,10). The pubic symphysis is not resistant to post-depositional processes, and estimates based on this area of the os coxa are less reliable and precise for individuals who die after the age of 40 because changes here are likely to reflect retarded maturation (15–17) and thus underestimate age at death for older specimens. The auricular surface belongs to a more conservative region and its age-related morphological modifications occur early and continue until the age of 60 (18,19). However, estimates based on observations of the auricular surface of adult specimens of known age and sex do not give very accurate results (20–22); estimates of age at death for the majority of individuals were between 30 and 50 years old, underestimating the age at death of individuals older than 50 years and overestimating the age of the younger individuals.

Recently, it has been proposed that changes in the region of the acetabulum occurring with age may be useful to estimate age at death in adults (23–26) and Rougé-Maillart et al. (27) found a high correlation between these changes and both the age at death and the auricular surface stages described by Lovejoy et al. (18). The possibility of using this conservative region on unknown skeletons increases the possibility of age assessment by the assignment of another age marker, but also allows the diagnosis of remains pertaining to wider age spectrum. In addition, the acetabulum is preserved longer in skeletal remains, therefore a method applied directly to this region would provide a relevant age marker. Fulfilling these aims could be very useful in Forensic Anthropology and in the study of ancient human remains opening, new possibilities. The main purpose of the work reported here was to describe age morphological changes of the fused acetabulum and analyze the potential to estimate adult age at death using its observations.

Materials and Methods

The material used was the documented skeletal collection of *Esqueletos Identificados* of Coimbra housed in the Department of Anthropology of the University of Coimbra (Portugal) formed by individual buried between late 19th and early 20th centuries (28). From this collection we selected male individuals for which the three elements of the os coxa were fused. We excluded individuals who showed pathologies in either acetabulum, but did not exclude those with noninflammatory osteoarthritis or diffuse idiopathic skeletal hyperostosis because these conditions are related to age (29,30). Therefore, a total of 242 male individuals from 16 to 96 years old was selected. Only the left os coxa was used.

The wide range of age represented by these specimens was used to reflect a more complete spectrum of the morphological changes that can occur in the region of the acetabulum throughout a human life span.

[1] Dept. de Antropologia, Facultad de Ciências, Universidad de Coimbra, 3000-056-Coimbra, Portugal.
[2] Unitat d'Antropologia, Dept. de Biologia Animal, Vegetal i Ecologia, Universitat Autònoma de Barcelona, 08193 Bellaterra, Spain.
[3] Deptment of Ecology and Evolution, University of Michigan, Ann Arbor, MI 48109-1048.

*Grant Sponsorship: research grant (SFRH/BPD/6075/2001) from Fundação para Ciência e a Tecnologia—Operational Program Science Technology and Innovation (POCTI) to C Rissech and the Sabbatical Leave Program of the University of Michigan, Ann Arbor to G. F. Estabrook.

Part of this work was presented as a poster in the 14th Congress of European Anthropological Association. Human Variability: A Bridge between Sciences and Humanities in Komotini, Greece (September 1–5, 2004). The title of the poster was "Acetabular Observations Enable Accurate Estimates of Age at Death of Adults over 40 years."

Received 13 Nov. 2004; and in revised form 16 April and 12 July 2005; accepted 21 July 2005; published 13 Feb 2006.

Description of Variables

To carry out our purpose, seven variables based on previous observations and work (24–27) were defined and later scored in the sample. These seven variables describe the area adjacent to the acetabulum, the rim of the acetabulum, the outer edge of the acetabular fossa, and the acetabular fossa. We did not use variables from the lunate surface because, in our preliminary analysis they displayed substantially lower significance and had greater overlap in age at death among states.

Each of seven variables was structured as a series of states describing the various kinds and extents of observed morphological conditions. The seven variables are (1) acetabular groove; (2) acetabular rim shape; (3) acetabular rim porosity; (4) apex activity; (5) activity on the outer edge of the acetabular fossa; (6) activity of the acetabular fossa; and (7) porosities of the acetabular fossa. The seven variables and their states are described accurately in Table 1 and illustrated with photographs (Figs. 1–38) to complement the descriptions. The descriptions refer to the anatomical structures shown in Fig. 1.

Appropriateness of the Variables

To argue the appropriateness of the variables and quantify correlation with age Kruskal–Wallis (31) and Kendal range (32) tests were calculated. Box plots of age at death within the states of each variable were also examined visually to identify the fraction of stages within a specific age range. Mean, standard error, and standard deviation have been considered.

Moreover, how the states of the variables specifically correspond to known age at death and intra- and inter-observer constancy were quantified. To quantify how the states of the variables specifically correspond to known age, the mean and the variance of known age at death were calculated for each state of each variable, a total of 41 states. To compare observed variance with how much variance would be expected if a state describing as many specimens were unrelated to age, a simulated state was assigned at random, and independent of age at death, to that same number of specimens. Variance among specimens simulated to have this state was calculated and compared with variance in known age at death among specimens in the observed state. This was repeated 1000 times. The number of simulated states with variance less or equal to the variance of the observed state is a measure of the significance of the relationship of the observed state with known age at death under the hypothesis that this state is independent of known age at death. The average variance over the 1000 simulated states can be compared with the variance in the observed state to determine "% squared error explained" in the context of the scored sample. Skew was calculated as the third moment about the mean. Skew indicates whether the greatest errors were over-estimates (positive) or under-estimates (negative), and its magnitude reflects the magnitude of these greatest errors, in units of years.

To quantify intraobserver constancy, 62 coxae were observed twice, at different times, three months apart, by the same observer. The constancy of observations was evaluated by Wilcoxon's test (33). To quantify interobserver constancy and evaluate the utility of the descriptions and photos of the seven variables, 38 coxae were observed, under identical conditions and using only the descriptions and photos, by three different observers with different osteological experience. One of the observers was a Ph.D student of Zooachaeology, another held a Master's degree in Anthropology, and the third was a Ph.D expert on coxae. Our intention was to evaluate also how an untrained but osteologically competent person could score the traits using only the information given in descriptions and photos of the variables. The constancy among the three data sets was evaluated using Friedman's test (33).

Analysis of the Accuracy of the Variables in Age Prediction

Our second goal is to analyze the accuracy of the variables. So that our results will be comparable with those of other workers, we used the same Bayesian method as Schmitt and Broqua (16), Lucy et al. (34), Schmitt et al., (35), and Gowland and Chamberlain (36). The computational details of this Bayesian estimation procedure are fully described in this journal by Lucy et al. (34). In our application, prior probability (the probability that the age at death of an unknown individual falls in an age class before any bones have been examined) is estimated as the fraction of individuals in the reference collection with known age at death in that age class. Thus, our underlying assumptions are that test individuals are at least 16 years old and are drawn from a population whose survivorship is similar to that of the reference collection.

The posterior probability (the probability that the age at death of an unknown individual falls in an age class after some bones have been examined) is based on conditional probability distributions of age (class) at death given that a particular osteological feature had been observed in the test specimen (37). These distributions were estimated by observing frequencies in the reference collection.

To ensure that our test specimens met our underlying assumptions, each specimen was removed, one at time, from the reference collection and used as a test specimen. After experimenting with age class widths from 3 to 10 years, we chose relatively narrow 5-year age classes because the variables we report here enabled us to estimate age with this precision, but with no substantial loss of accuracy. Thus, we report results here based on 5-year age classes.

We can associate with a probability distribution, the expected value of the central age in each class to determine a single age estimate (estimated age). One measure of the accuracy of an estimate is the absolute difference between this expected value and known age at death. Even when estimated age is close to known age at death, another kind of estimation inaccuracy occurs when incorrect age classes are given moderately high probabilities. A measure of this inaccuracy, called fit, is the expected value of the absolute difference between the known age and the nearest age in any age class (except the one in which the known age falls). Fit shows how closely the estimating distribution fits known age at death.

Although, the computational details of this Bayesian estimation procedure are fully described by Lucy et al. (34), this study has been implemented with a computer program (IDADE2) with which we developed the calculations of the present study. The explanation of the calculations and the IDADE2 program can be downloaded from http:\\www-Personal.umich.edu\~gfe\, where many other computational applications can also be found.

Results

For clarity, the results of the appropriateness and accuracy analysis of the variables will be considered individually.

Appropriateness of Variables

Kruskall–Wallis statistics to quantify the correlation of each variable with known age at death were all significant. The seven variables had substantially higher values (all >120) for this test

TABLE 1—*Morphological description of the seven acetabular variables and their states.*

Variable	Description of the Variable	States of the Variable	Characteristics of the States	Code
(1) Acetabular groove	This groove appears below and surrounds the internal margin of the acetabular rim. With age, the acetabular groove can become more or less pronounced either along the entire acetabular rim or along only a part of it	No groove (Fig. 2)	There is no groove below the acetabular rim. There is no anatomical interruption between the lunate surface and the acetabular rim	0
		Groove (Fig. 3)	An anatomical interruption is observed between the lunate surface and the acetabular rim. Although it might be short or shallow, it surrounds some or much of the acetabular rim	1
		Pronounced groove (Fig. 4)	A deeper groove surrounds a large part of the acetabular rim	2
		Very pronounced groove (Fig. 5)	An extremely pronounced groove surrounds nearly all the acetabular rim. In some specimens, extreme growth of the rim has obscured the groove so that only a tissue discontinuity between the lunate surface and the acetabular rim can be observed	3
(2) Acetabular rim shape	With age, the acetabular rim losses its round and smooth form as a consequence of the progressive development of osteophytes, which can become a crest	Rounded acetabular rim (Fig. 6)	The acetabular rim is dense, round and smooth, typical of young specimens	0
		Partially narrow acetabular rim (Fig. 7).	The acetabular rim keeps its round and smooth form in some areas but in others is narrower. There are two possibilities: (a) the iliac part of the acetabular rim narrows but not the ischial part; or (b) the external part of the acetabular rim retains its rounded form but its internal part has an upright form. In all of these cases, the acetabular rim is smooth to the touch	1
		Narrow or rough acetabular rim (Fig. 8)	There are two possibilities: (a) whole acetabular rim is narrow, or (b) some part of the acetabular rim might be rough to the touch due to the presence of little grooves. In both possibilities, there is no osteophytic construction	2
		Partially crested rim (Fig. 9)	Osteophytic constructions form a small chain ($\approx$ 1 mm in height) on some small part of rim; a bigger osteophyte linked or not to the chain might be observed	3
		Crested rim (Fig. 10)	An osteophytic formation makes either (a) a low crest ($\approx$ 1 mm in height) along the entire acetabular rim or (b) a high crest (2–4 mm in height) along only part of it. This crest appears dense	4
		Very high crested rim (Fig. 11)	A very high crest ($>$ 4 mm in height) has developed as a consequence of bone construction and destruction. This crest is thin and sharp or rounded with a spongy appearance	5
		Destructured rim (Fig. 12)	An extremely high crest ($>$ 8 mm in height) has developed. It may be either thin and sharp and leaning slightly toward the lunate surface, or rounded, spongy and fragile with swollen and hollow bone	6
(3) Acetabular rim porosity	With aging, porosity appears on the acetabular rim and on the adjacent ilio-ischiatic area of the acetabulum. Two kinds of porosity can be defined: (a) micorporosity, which refers to a fine, just optically visible perforation ($\leq$ 1 mm); and (b) macroporosity, which refers to an oval or round perforation larger than 1 mm	Normal porosity (Fig. 13)	Acetabular rim is smooth without porosities and roughness. The area adjacent to the acetabular rim also has normal porosity	0
		External porosity (Fig. 14)	On the area around the acetabulum, microporosity is lightly increased on the anterior inferior iliac spine, on the posterior wall of the acetabulum and on the area below the two extremities of the lunate surface. There is no porosity on the acetabular rim, which is dense and smooth	1
		Rim porosities (Fig. 15)	Some microporosities on the acetabular rim may be large (= 1 mm) but the acetabular rim always has a round and dense appearance. There is no bone destruction	2
		Rough rim (Fig. 16)	The acetabular rim is not smooth to the touch and there may be some macroporosity on the rim	3
		Destructured rim (Fig. 17)	Newly constructed bone has become very porous with many micro- and macroporosites, or it has suffered subsequent destruction	4
		Extremely destructured rim (Fig. 18)	Macro- and microporosities of the destructured acetabular rim have partially invaded the lunate surface. Usually this invasion occurs on the superior area of the lunate surface below the anterior inferior iliac spine	5

TABLE 1—*Continued*

Variable	Description of the Variable	States of the Variable	Characteristics of the States	Code
(4) Apex activity	Apex activity refers to the bone activity observed on the apex of the posterior horn of the lunate surface. With aging, this apex loses its rounded form, gradually becoming sharper and finally developing a spicule, which can become quite large	No activity (Fig. 19)	The apex is round and smooth to the touch. There is no spicule	0
		Apex activity (Fig. 20)	The apex has become longer and is sharp to the touch, or a small spicule can be felt	1
		Osteophytic activity (>1 mm) (Fig. 21)	A developed and conspicuous osteophyte larger than 1 mm can be seen with the naked eye	2
		Much osteophytic activity (>3 mm) (Fig. 22)	The apex has an osteophyte larger than 3 mm, which may cover the entire horn of the lunate surface	3
		Very much osteophytic activity (>5 mm) (Fig. 23)	An osteophyte is so large (>5 mm) that it enters the acetabular notch and may completely cross it, in which case the anterior horn of the lunate surface also has activity	4
(5) Activity on the outer edge of the acetabular fossa	This activity refers to an osteophytic formation that grows as a mini-crest from the outer edge of the acetabular fossa towards the lunate surface. Usually, it can be felt but not seen. When it is present, the edge is rough to the touch and can be detected by repeatedly moving the finger along the outer edge of the acetabular fossa towards the acetabular fossa surface (Fig. 24). Sometimes this osteophytic formation becomes visible and extensive enough to cover the acetabular fossa	No activity on the outer edge	The outer edge feels smooth, or at least not rough, and the finger moves smoothly over it towards the fossa	0
		Slight activity ($<1/4$) on the outer edge	A mini-crest can be felt (but not seen) on less than one quarter of the outer edge of the acetabular fossa. It is usually found on only one of the two horns of the lunate surface, near the apex	1
		Medium activity ($<1/2$) on the outer edge	Bone growth can be felt (but not seen) on between a quarter and half of the outer edge of the acetabular fossa. Usually, this bone growth is not continuous; therefore, all the active parts must be considered to estimate the proportion	2
		Much activity ($<3/4$) on the outer edge	Bone growth can be felt on between one half and three quarters of the outer edge of the acetabular fossa	3
		Extreme activity ($>3/4$) on the outer edge	Bone growth can be felt and sometimes it can be seen on more than three quarters of the outer edge	4
		Destructured outer edge (Fig. 25)	There is so much visible bone growth on the outer edge towards the fossa that it partially covers the fossa parallel to the outer edge	5
(6) Activity of the acetabular fossa	The young acetabular fossa appears dense and smooth and is almost level with the lunate surface. With aging, the acetabular fossa moves to a more internal position and clearly appears deeper than the lunate surface. Also the activity, expressed as relief, porosities, and bone production, is present on the fossa. When this activity is extreme, the acetabular fossa may be obliterated	No activity (Fig. 26)	The lunate surface is level with the acetabular fossa, which appears dense and smooth	0
		Slight activity (Fig. 27)	The lunate surface is clearly no longer level with the acetabular fossa, which still appears dense and smooth	1
		Peripheral activity (Fig. 28)	The acetabular fossa shows activity on between a quarter and a half of its surface. This activity is usually located on the posterior area of the fossa or sometimes on peripheral areas, but never on the center. This activity results in relief, porosities and spongy bone, which grows toward the lunate surface from small parts of the external border of the fossa. Areas of the acetabular fossa without activity appear dense and smooth	2

TABLE 1—*Continued*

Variable	Description of the Variable	States of the Variable	Characteristics of the States	Code
		Central activity (Fig. 29)	There is activity on about half of the fossa. It is usually found on the posterior half and always extends to the center. Activity on the center of the acetabular fossa usually produces a relief that is similar to the trabeculae. Peripheral activity is usually expressed by porosities. There may be some growth of spongy bone toward the lunate surface	3
		Major activity (Fig. 30)	Activity is observed on more than three quarters of the fossa. This activity produces relief and porosities, but the fossa does not lose its consistency and density	4
		Generalized activity	The entire fossa, or nearly all of it, is covered by extensive formation. There are two possibilities: (a) the fossa is not consistent nor dense (Fig. 31*a* and *b*) the fossa is partially or totally obliterated (Fig. 31*b*)	5
(7) Porosities of the acetabular fossa	Through the aging process, microporosities first become macroporosities, then trabecular bone, and finally destruction invades the entire fossa. There are two types of macroporosities. (1) Smaller ($\leq$1.5 mm) macroporosities occur as a transition of micoporosities into trabecular bone; these have a blunt perimeter and will be called smaller macroporosities. (2) Larger (>1.5 mm) macroporosities have a sharp perimeter due to destruction; these are conspicuous, larger and either round or less regular and will be called macroporosities with destruction	Dense acetabular fossa (Fig. 32)	The acetabular fossa is dense and smooth, but it may have a few normal peripheral microporosities	0
		Acetabular fossa with microporosties (Fig. 33)	The acetabular fossa appears dense but there are small areas with some microporosities. These areas look like "orange skin," usually on the superior lobe of the fossa, but sometimes elsewhere	1
		Macroporosities or peripheral trabecular bone	Part of the fossa is covered with microporosities and smaller macroporosities. These porosities occur on about one half of the fossa, which can include the center, but not on all three lobes (Fig. 34*a*). Some trabecular bone may occur on the peripheral area of the fossa (Fig. 34*b*)	2
		Macroporosities on the three lobes (Fig. 35)	Porosities occur on about three quarters of the fossa. The three lobes and the center of the fossa are covered with smaller macroporosities and microporosities, but not the area of the acetabular notch. Trabecular bone may occur on the peripheral area of the fossa	3
		Macroporosities with destruction (Fig. 36)	Macroporisities with destruction occur on a base of microporosities and smaller macroporosities. This may be observed over most of the fossa or only over a restricted area	4
		Bone destruction on most of the fossa (Fig. 37)	Most of the fossa is covered with trabecular bone. There are no microporosities. There is much destruction evidenced by large irregular macroporosities with destruction. The bone of the fossa is swollen and has lost consistency as a result of bone destruction	5
		Bone proliferation (Fig. 38)	Bone proliferation on the acetabular fossa obliterates the fossa	6

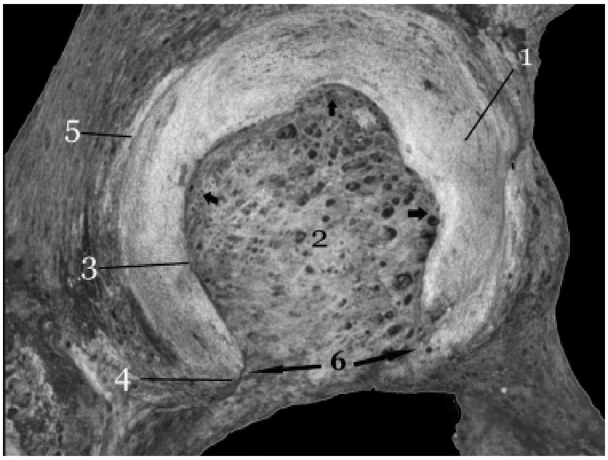

FIG. 1—*Terminology. 1, The lunate surface. This is the articular surface within the acetabulum. 2, The acetabular fossa. This is the nonarticular surface within the acetabulum. The three arrows in this area indicate the three lobes of the fossa. 3, The outer edge of the acetabular fossa. This is the limit between the lunate surface and the acetabular fossa. 4, The apex of the posterior horn of the lunate surface. 5, The acetabular rim surrounding the acetabulum. 6, The acetabular notch. It is compressed between the two horns of the lunate surface (arrows).*

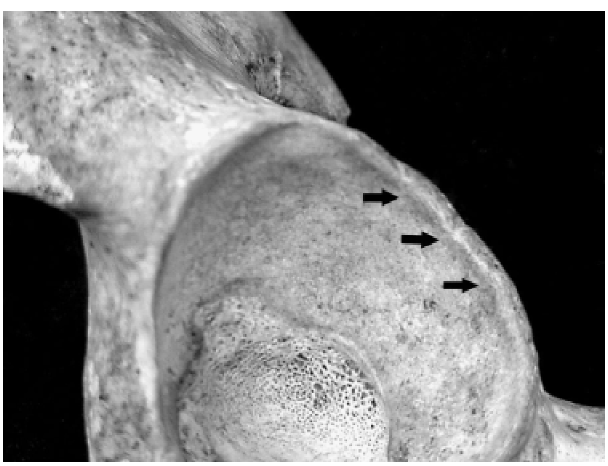

FIG. 2—*State 0 of variable 1 (♂, 17 years). There is no groove (arrows) below the acetabular rim.*

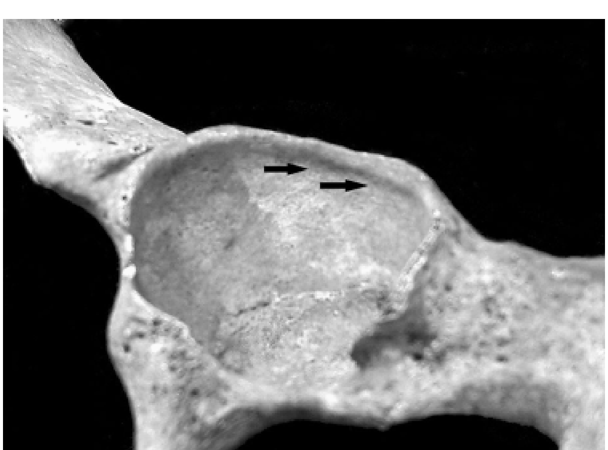

FIG. 3—*State 1 of variable 1 (♂, 28 years). The arrows point to a noticeable groove below some of the acetabular rim.*

FIG. 4—*State 2 of variable 1 (♂, 44 years). The arrows point to a pronounced groove below the ilio-ischiatic area of the acetabular rim.*

statistic (Table 2). Box plots (Fig. 39) of the variables show the fraction of states in a specific age range, indicating mean, standard error, and standard deviation. The age ranges of the states of each variable cover all individual ages from young to old and with only slight overlap. In addition, Bayesian inference increases accuracy by using all the variables simultaneously.

The analysis of how the states of the variables specifically correspond to known age (Table 3) shows that 38 of the 41 states, except for the three states with fewer than 10 specimens, were significantly correlated with known age and 35 of them were significant at $p < 0.005$. Within each variable, mean known ages of

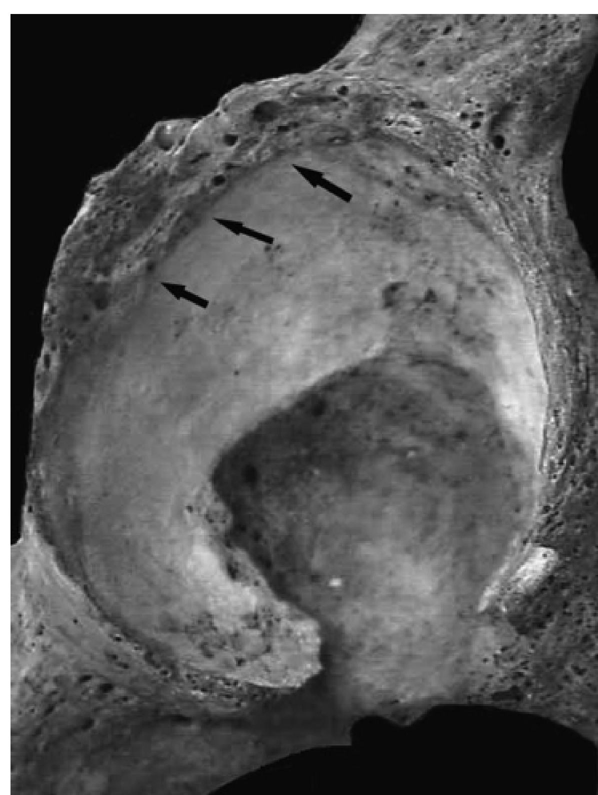

FIG. 5—*State 3 of variable 1 (♂, 63 years). Extremely pronounced interruption (tissue discontinuity) between the lunate surface and the acetabular rim (arrows) surrounding nearly all the acetabular rim.*

FIG. 6—*State 0 of variable 2 (♂, 16 years). The arrows point to the dense, round and smooth acetabular rim.*

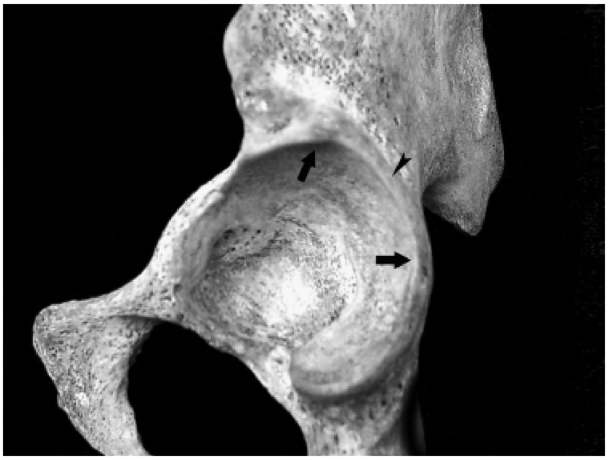

FIG. 7—*State 1 of variable 2 (♂, 27 years). The external part of the acetabular rim is rounded (arrowhead) and the internal part has an upright form (arrows). This image corresponds to the 1b category of this variable.*

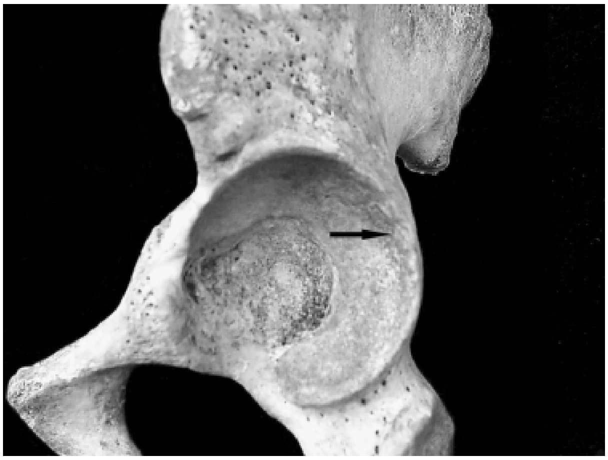

FIG. 8—*State 2 of variable 2 (♂, 22 years). Narrow acetabular rim with surface rough to the touch on it posterior part, where the arrow points to some slight roughness. This image corresponds to the 2b category of this variable.*

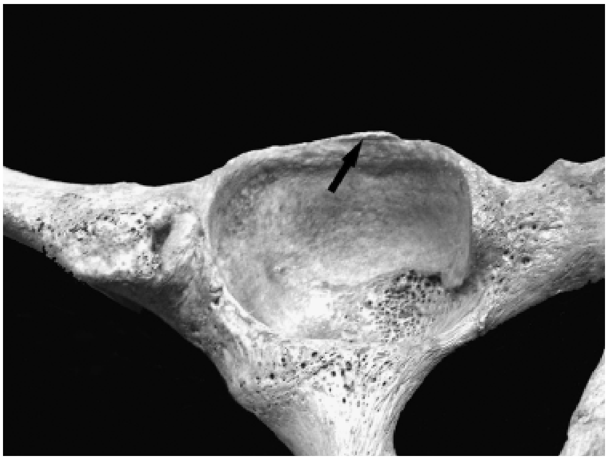

FIG. 9—*State 3 of variable 2 (♂, 31 years). osteophytic construction forming a small chain 1 mm in height on the posterior part of the acetabular rim.*

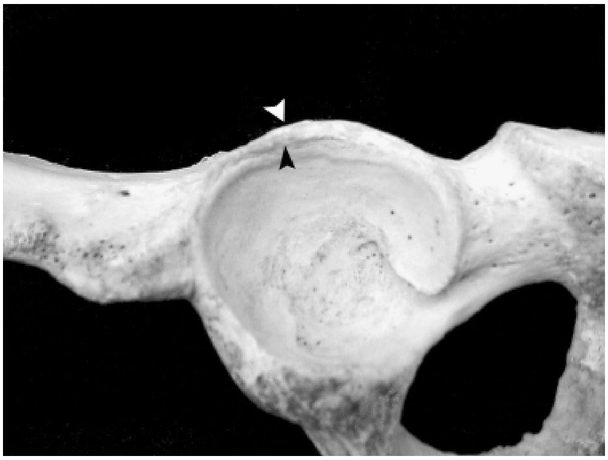

FIG. 10—*State 4 of variable 2 (♂, 63 years). A high (4 mm) dense crest along just the posterior area of the acetabular rim is shown between arrow heats. This image corresponds to the 4 b category of this variable.*

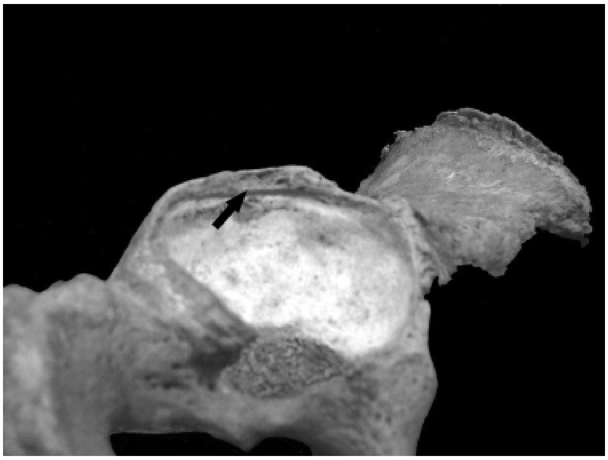

FIG. 11—*State 5 of variable 2 (♂, 69 years). A very high (5 mm) and sharp crest on most of the acetabular rim.*

FIG. 12—*State 6 of variable 2 (♂, 73 years). Arrows point to a destructured acetabular rim with an extremely high (1 cm) crest all around.*

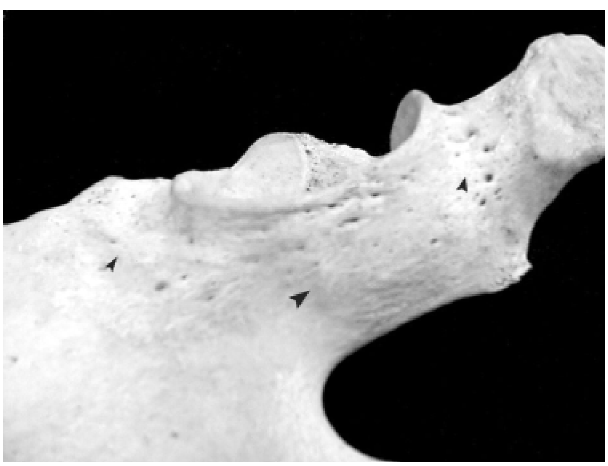

FIG. 13—*State 0 of variable 3 (♂, 27 years). Smooth acetabular rim without porosities. Arrowheads point to normal porosity on the adjacent area of the acetabular rim.*

FIG. 14—*State 1 of variable 3 (♂, 27 years). Arrowheads show where microporosity has increased on the posterior wall of the acetabulum. There is no porosity on the acetabular rim.*

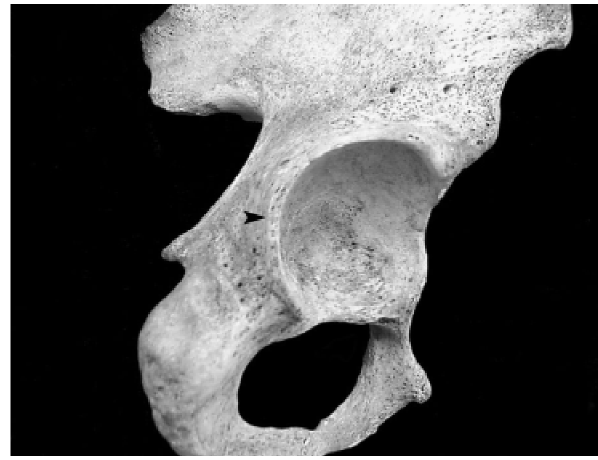

FIG. 15—*State 2 of variable 3 (♂, 27 years). There are some large and small microporosities on the ischiatic part of the acetabular rim. The acetabular rim appears round.*

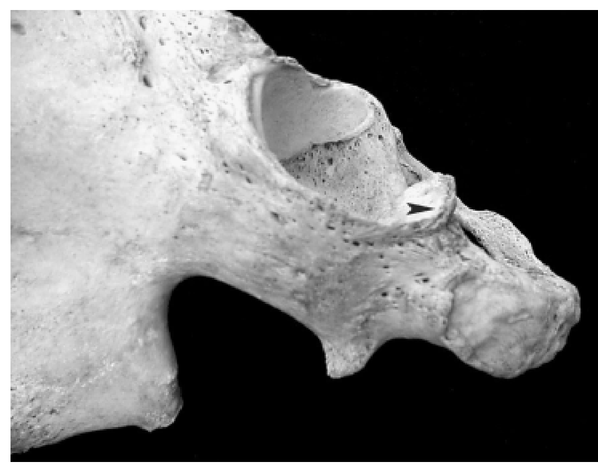

FIG. 16—*State 3 of variable 3 (♂, 53 years). Not all the acetabular rim is smooth to the touch. The arrows point to some roughness on it.*

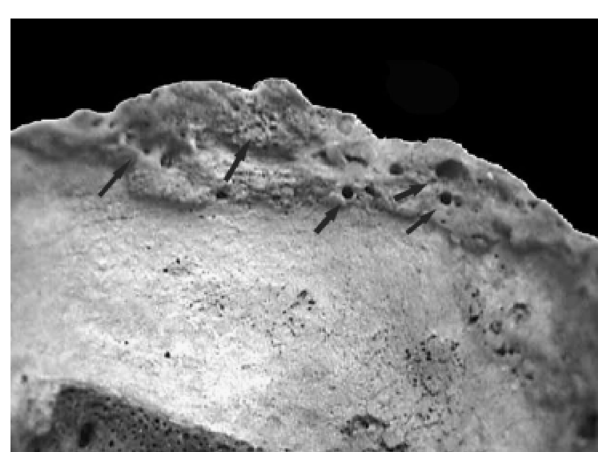

FIG. 17—*State 4 of variable 3 (♂, 63 years). The acetabular rim appears fragile because of its great porosity. Micro- and macroporosity are evident.*

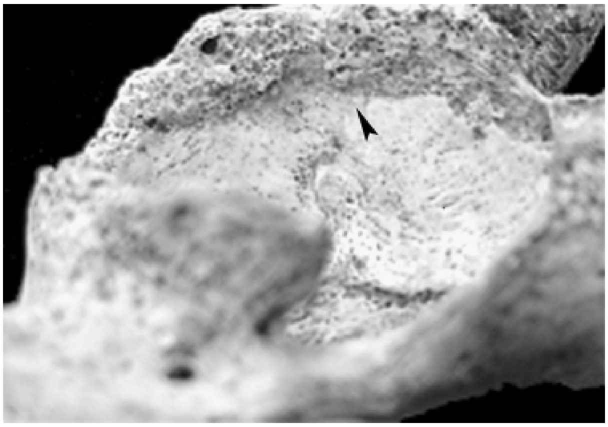

FIG. 18—*State 5 of variable 3 (♂, 63 years). The extreme macro- and microporosity of the destructured acetabular rim invade the superior area of the lunate surface.*

FIG. 19—*State 0 of variable 4 (♂, 18 years). The apex of the posterior horn of the lunate surface is round and smooth (arrow). There is no spicula.*

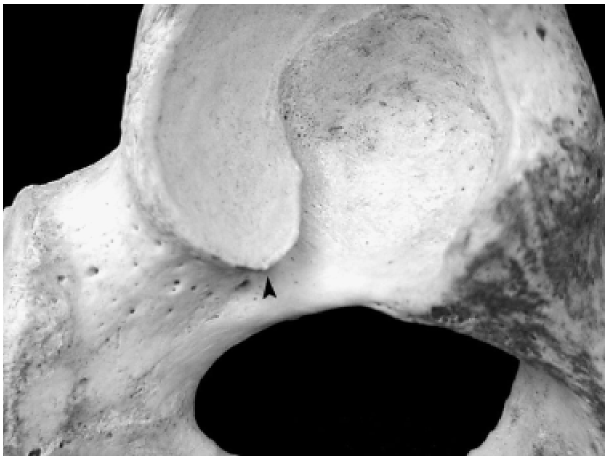

FIG. 20—*State 1 of variable 4 (♂, 63 years). The arrows point to where a small spicula could be felt on the apex of the posterior horn of the lunate surface.*

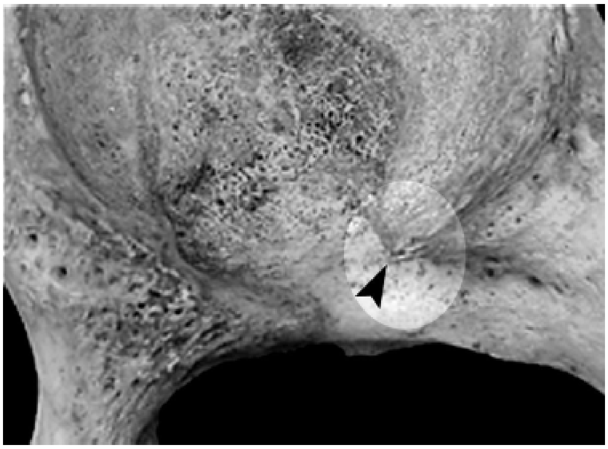

FIG. 21—*State 2 of variable 4 (♂, 53 years). The arrow points to a conspicuous osteophyte larger than 1 mm.*

FIG. 22—*State 3 of variable 4 (♂, 55 years). An osteophyte larger than 3 mm covers the entire posterior horn of the lunate surface (arrow).*

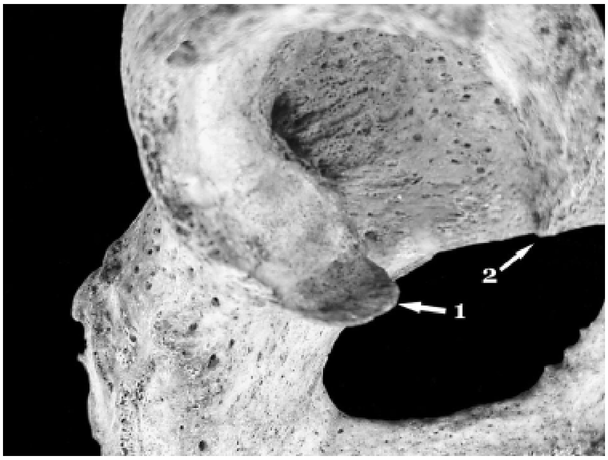

FIG. 23—*State 4 of variable 4 (♂, 63 years). An extremely large osteophyte (>5 mm) is on the posterior horn of the lunate surface (arrow 1). In this case, the anterior horn also shows bone growth (arrow 2).*

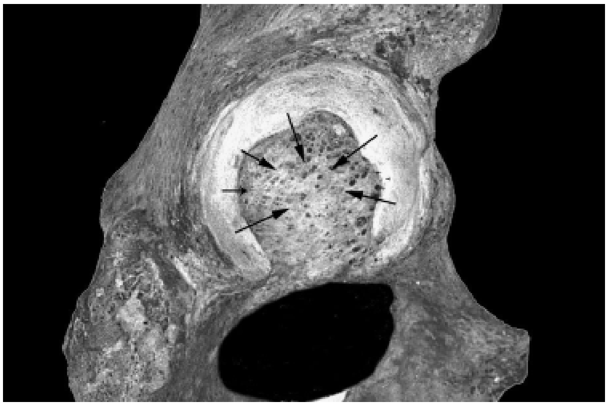

FIG. 24—*Variable 5. The arrows indicate how to move the finger along the outer edge of the acetabular fossa towards the fossa.*

FIG. 25—*State 5 of variable 5 (♂, 73 years). Extreme growth of the outer edge towards the fossa, which is partially obliterated (arrow).*

FIG. 27—*State 1 of variable 6. (♂, 18 years). The acetabular fossa is still dense and smooth, but no longer level with the lunate surface (arrows).*

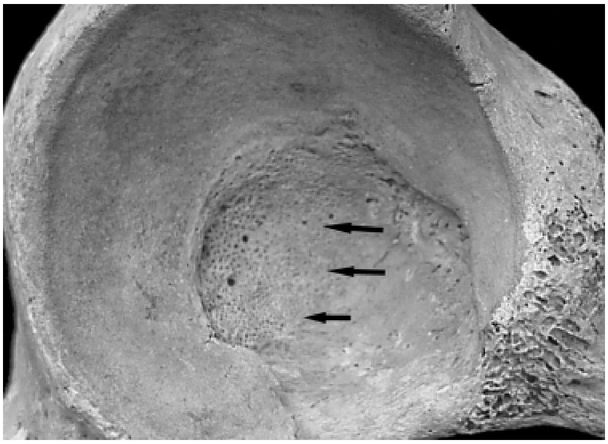

FIG. 28—*State 2 of variable 6 (♂, 26 years). Activity on less than a half of the fossa (arrows). The activity is only on the posterior half and does not extend to the center of the fossa.*

death within states are separated and spread over much of the range observed among specimens.

None of the seven variables showed significant intra- and interobserver differences between different observers or times, except for one slight but nonsignificant difference in how two of the three observers scored the second variable. These seven variables seem to have states and descriptions that can be consistently observed for an untrained but osteologically competent person.

These results indicate the appropriateness of the variables for age estimation.

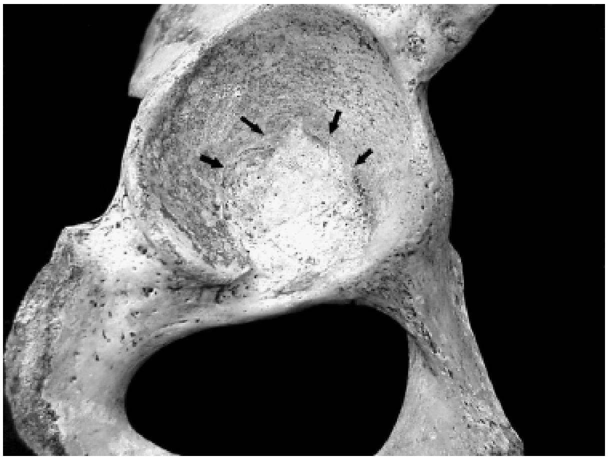

FIG. 26—*State 0 of variable 6 (♂, 19 years). The fossa is level with the lunate surface (arrows).*

FIG. 29—*State 3 of variable 6 (♂, 19 years). Activity on the posterior half of the fossa and extending to the center (arrows).*

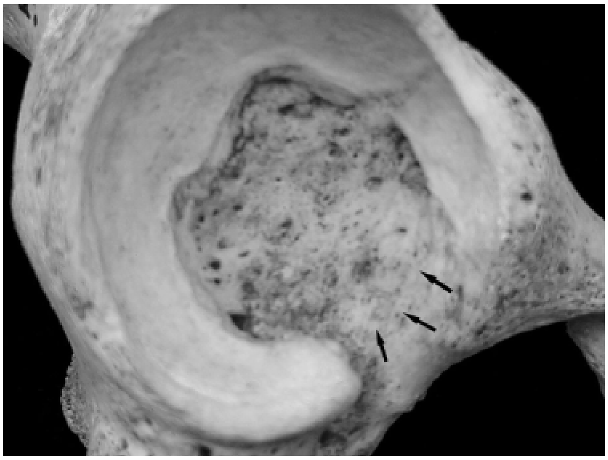

FIG. 30—*State 4 of variable 6 (♂, 39 years). Activity on more than three quarters of the fossa (arrows). The fossa is consistent.*

FIG. 32—*State 0 of variable 7 (♂, 18 years). The acetabular fossa is dense and smooth, with normal porosity.*

Analysis of the Accuracy of the Variables in Age Prediction

Estimates of age at death for a few example specimens, showing the known age at death, the estimating probability distribution over age classes, expected age at death calculated from this distribution, and the measure of fit is presented in Table 4.

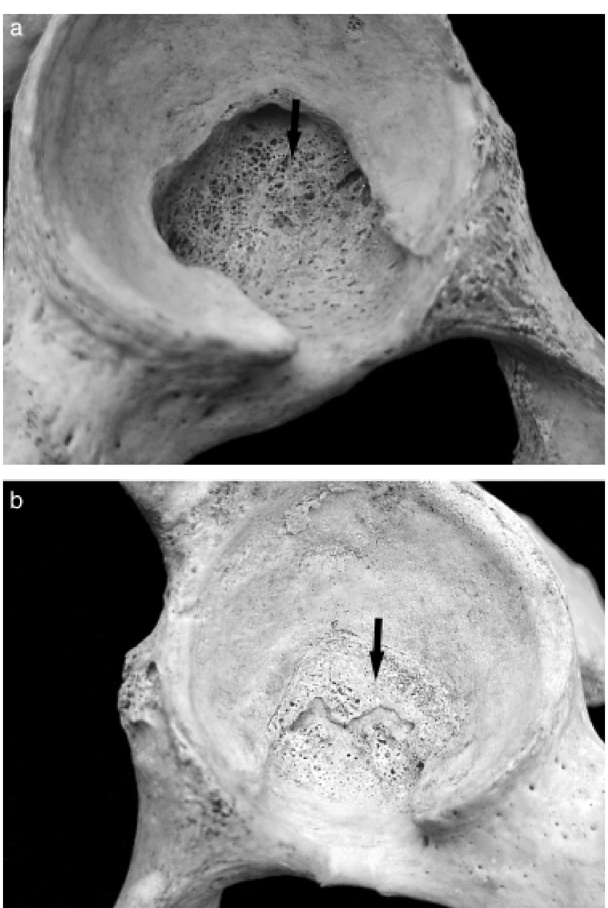

FIG. 31—*State 5 of variable 6 (a) (♂, 46 years). The bone of the fossa has lost its consistency. (b) (♂, 45 years) The fossa is partially obliterated as a consequence of extensive bone formation.*

The difference between known age and the estimated age (Table 5) is within 10 years in more than 89% of the specimens. About 67% received estimates within 5 years and nearly 35% received estimates within 2 years of known age at death.

The fit value (Table 6) shows that over 60% of the specimens had an expected difference between known age at death and the estimating distribution of less than 5 years, and only about 11% received values of fit over 10 years.

Results (Tables 5 and 6) clearly show that these measures of accuracy do not vary widely with age, indicating that these variables might be expected to estimate age at death with nearly equal accuracy over all adult ages.

Discussion

The first descriptions of the relationship between morphological changes of the acetabulum and age at death of an individual were given by Rissech and Malgosa (23), Rissech (24), and Rissech et al. (25), who observed changes on the acetabular fossa. Later, Rougé-Maillart (26), and Rougé-Maillart et al. (27) described more of these changes and demonstrated their correlation with the stages of auricular surface described by Lovejoy et al. (18). In this

FIG. 33—*State 1 of variable 7 (♂, 19 years). Dense acetabular fossa with some microporosities on the superior and posterior lobes (arrows).*

FIG. 34—*State 2 of variable 7 (a) (♂, 27 years). Arrows point to a macroporosity and the arrowhead points to a microporosity. In this case the macroporosity has a blunt perimeter and is beginning to transform to trabecular bone. (b) (♂, 23 years). The arrow points to some trabecular bone on the peripheral area of the fossa.*

article, we have described and ordered categories for seven variables of age at death to make this aging process explicit in three anatomical zones of the acetabulum: the acetabular rim; the outer edge of the acetabular fossa; and the acetabular fossa. Changes of the morphology of the lunate surface are not so well correlated

FIG. 35—*State 3 of variable 7 (♂, 25 years). There are macro- and microporosity on all three lobes and the center of the fossa (arrows). There is no porosity on the external area of the acetabular notch.*

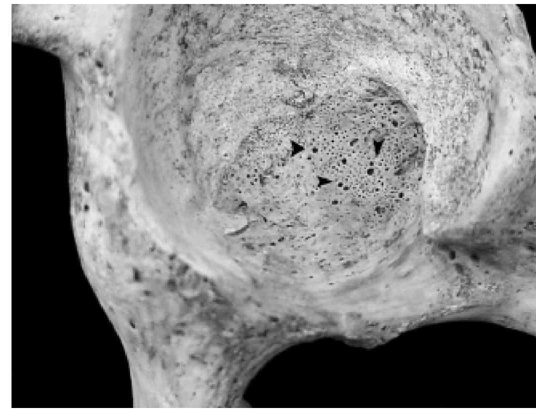

FIG. 36—*State 4 of the variable 7 (♂, 41 years). The acetabular fossa has a base of micro- and macroporosities dotted with macroporosities with destruction, indicated by arrows.*

FIG. 37—*State 5 of variable 7 (♂, 35 years). Trabecular bone occupies most of the fossa.*

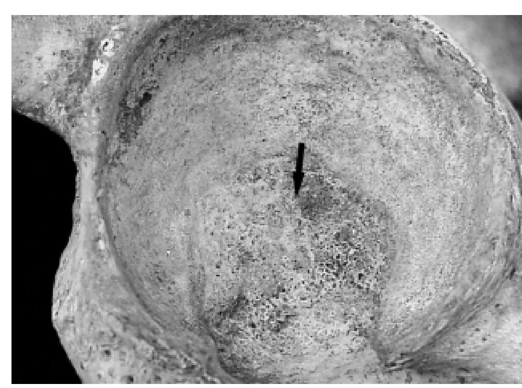

FIG. 38—*State 6 of variable 7 (♂, 53 years). The fossa has been obliterated because of bone production in this area.*

TABLE 2—*Correlation between variables and age by Kruskal–Wallis test.*

Variable	Kruskal–Wallis Test	p (Statistical Significance)
Acetabular groove	120,892	0.000*
Thinning and bone construction of the acetabular rim	170,964	0.000*
Porosity and bone destruction of the acetabular rim	160,016	0.000*
Apex activity	126,858	0.000*
Activity of the outer edge	162,346	0.000*
Activity of the accetabular fossa	136,301	0.000*
Porosities of the acetabular fossa	175,060	0.000*

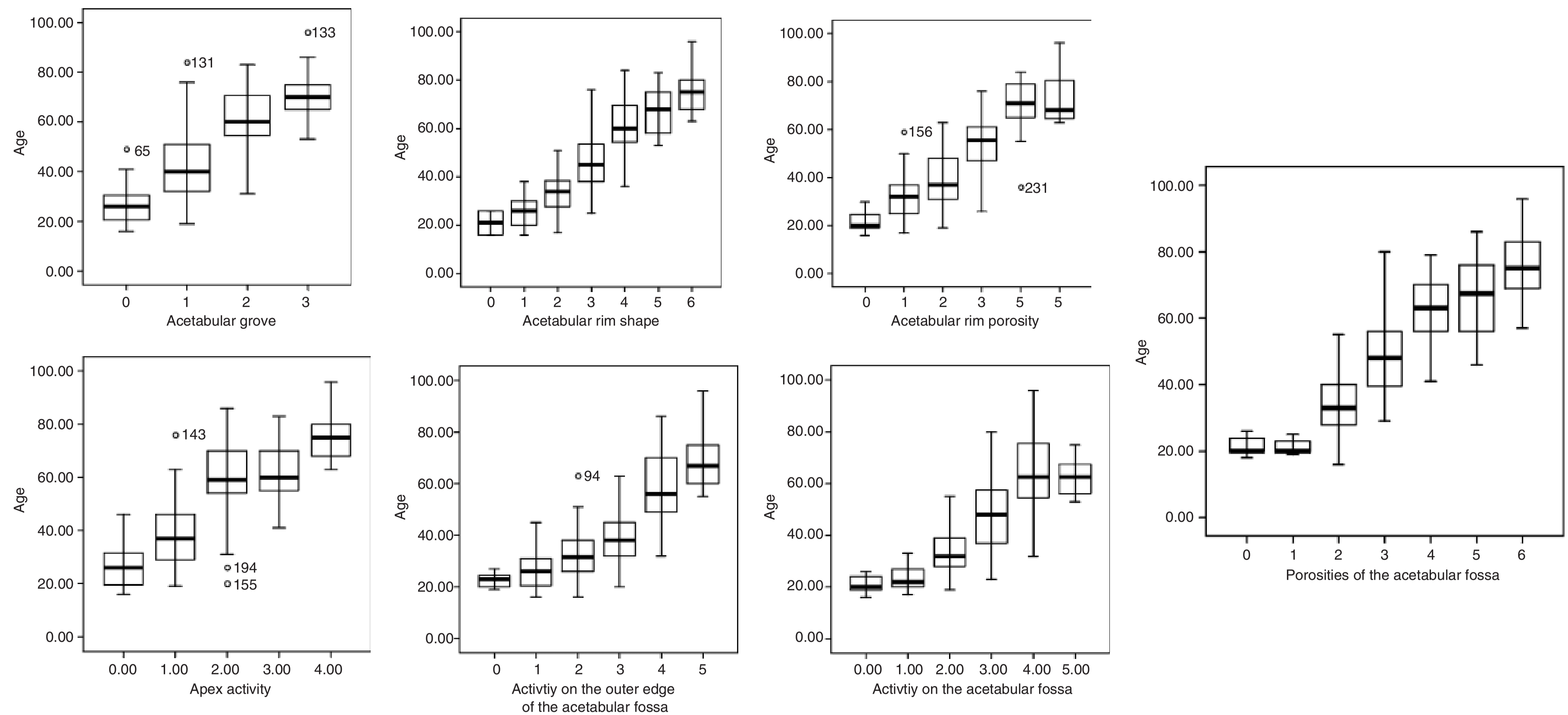

FIG. 39—*Box plot between age and each of the seven variables showing the relationship between each state of each variable (horizontal axis) with age (vertical axis). The central line indicates the mean, the box represents the standard error, and the whiskers correspond to the standard deviation.*

TABLE 3—*Results of the analysis of how the states of the variables specifically correspond to known age.*

State Variable	0	1	2	3	4	5	6
1							
n	39	138	43	22			
Mean	26.9	41.6	50.1	71.2			
Variance	7.45	13.58	13.13	9.49			
Skew	6.86	10.81	− 9.40	7.91			
%SE	81.9	41.0	43.7	70.3			
Significance	0.000*	0.000*	0.001*	0.000*			
2							
n	2	47	43	76	47	18	9
Mean	21.0	25.6	34.7	45.9	60.3	68.1	75.8
Variance	5.00	5.48	8.54	11.53	11.13	9.47	10.09
Skew	0.00	3.59	4.70	9.01	− 6.37	2.44	8.46
%SE	83.9	90.3	76.5	57.3	60.1	69.8	63.4
Significance	0.322	0.000*	0.000*	0.000*	0.000*	0.000*	0.050*
3							
n	15	57	65	72	26	7	
Mean	21.5	31.1	39.0	55.3	69.7	73.9	
Variance	4.21	8.22	10.74	11.61	10.76	11.75	
Skew	3.67	7.48	7.05	− 4.34	− 11.14	11.08	
%SE	94.0	78.5	63.0	56.3	61.7	48.6	
Significance	0.000*	0.000*	0.000*	0.000*	0.000*	0.147	
4							
n	28	129	55	21	9		
Mean	26.6	38.2	59.4	65.8	75.3		
Variance	7.93	11.97	14.38	10.03	9.85		
Skew	7.25	10.15	− 12.36	5.45	8.64		
%SE	79.1	54.5	37.6	66.6	65.6		
Significance	0.000*	0.000*	0.008*	0.001*	0.037*		
5							
n	7	23	60	47	78	27	
Mean	22.6	27.2	32.3	39.2	58.3	67.9	
Variance	2.87	7.98	9.33	9.89	12.56	9.94	
Skew	1.9	7.24	8.34	7.42	6.58	9.43	
%SE	96.9	78.9	71.9	68.3	49.3	67.5	
Significance	0.000*	0.000*	0.000*	0.000*	0.000*	0.000*	
6							
n	16	13	53	108	44	8	
Mean	21.0	23.3	33.9	48.1	63.8	62.5	
Variance	3.18	4.41	8.33	14.27	14.27	7.14	
Skew	1.65	3.81	6.88	9.14	− 6.56	4.91	
%SE	96.6	93.3	77.5	34.9	34.1	81.5	
Significance	0.000*	0.000*	0.000*	0.001*	0.018*	0.005*	
7							
n	13	9	100	47	46	22	5
Mean	21.4	21.6	34.3	48.7	62.7	67.5	76.0
Variance	2.59	2.17	8.92	10.95	9.53	11.48	13.11
Skew	2.29	1.18	6.18	8.94	− 6.86	− 5.31	6.11
%SE	97.7	98.3	74.6	61.1	70.6	56.4	32.9
Significance	0.000*	0.000*	0.000*	0.000*	0.000*	0.006*	0.334

For each variable and state, from top down is shown the number of specimens described by that state, mean age of those specimens, variance, skew, percent squared error explained and its significance under the hypothesis that any specimen is any age.

TABLE 4—*Estimates of age at death for a few example specimens.*

AD	EAD	FIT	15	20	25	30	35	40	45	50	55	60	65	70	75
16	19.9	3.3	62	20	18										
16	17.2	0.2	97	2	1										
21	22.6	0.8	1	86	13										
21	22.5	0.9	3	84	13										
23	31.4	8.4		3	34	37	24	2							
23	28.9	5.9		6	54	36	4								
31	31.4	1.7		7	9	74	8	2							
31	30.3	1.8		11	15	71	2	1							
54	49.8	3.8					1	5	38	51	1	4			
54	53.2	1.7						3	4	68	18	7			
68	64.5	5.9									36	11	31	15	7
68	68.5	5.0									19		26	41	14

Estimate for right side is above estimate for left side of same individual. Columns are labeled as follows: AD is known age at death; EAD is estimated age at death; FIT is expected difference between estimating distribution and AD; and 15, 20 . . . are the estimated probabilities of age class 15–19, 20–24 . . . in percent.

TABLE 5—*Number of specimens with absolute difference (|d|) between known age and estimated age, less than specified amounts, tabulated within age classes, and over all specimens.*

	|d| < 1			|d| < 2			|d| < 3			|d| < 4			|d| < 5			|d| < 10			|d| < 10				
Age		−	+		−	+		−	+		−	+		−	+		−	+		−	+	Nonestimated	Total
15–19	5	1	4	6	1	5	7	1	6	7	1	6	7	1	6	9	1	8	0	0	0	0	9
20–24	3	0	3	6	2	4	14	3	11	17	5	12	17	5	12	20	5	15	1	0	1	0	21
25–29	3	1	2	7	3	4	9	4	5	13	5	8	15	7	8	23	9	14	2	0	2	1	26
30–34	7	5	2	15	7	8	18	8	10	22	10	12	23	11	12	25	12	13	0	0	0	0	25
35–39	4	3	1	7	5	2	10	6	4	14	8	6	17	5	7	24	14	10	1	0	1	1	26
40–44	3	2	1	7	5	2	9	6	3	11	6	5	13	8	5	18	11	7	3	0	3	0	21
45–49	7	1	6	9	2	7	12	5	7	15	8	7	15	8	7	18	10	8	1	1	0	0	19
50–54	3	2	1	7	3	4	10	5	5	11	5	6	11	5	6	15	8	7	3	3	0	0	18
55–59	2	1	1	3	2	1	3	2	1	5	2	3	8	2	6	15	4	11	5	1	4	1	21
60–64	1	1	0	3	2	1	3	2	1	4	2	2	7	2	5	9	2	7	4	4	0	0	13
65–69	2	1	1	4	1	3	5	1	4	8	2	6	11	2	9	12	3	9	1	1	0	0	13
70–74	2	1	1	5	4	1	7	5	2	9	7	2	9	7	2	11	8	3	1	1	0	0	12
75–79	0	0	0	0	0	0	1	1	0	1	1	0	1	1	0	7	7	0	3	3	0	1	11
80–84	1	0	1	3	2	1	3	2	1	3	2	1	4	3	1	4	3	1	1	1	0	0	5
85–89	1	0	1	1	0	1	1	0	1	1	0	1	1	0	1	1	0	1	0	0	0	0	1
90–94	0	0	0	0	0	0	0	0	0	0	0	0	0	0	0	0	0	0	0	0	0	0	0
95–99	1	0	1	1	0	1	1	0	1	1	0	1	1	0	1	1	0	1	0	0	0	0	1
Total	45			84			113			142			160			212			26			4	242

Number of individuals underestimated (−) and overestimated (+) within and specific absolute difference.

with known age of death among the specimens; these changes in morphology may involve unknown factors unrelated to age. These unknown factors might include taphonomic factors, such as the tendency of humidity to increase the porosity of osteological remains (38,39), or they might include differences in acetabular morphology and body weight, which affect the articulating surfaces to differentially modify the area of contact between the lunate surface and the femoral head, resulting in different patterns of wear on the surface of the acetabulum over the same time periods (40).

The processes of change described by the seven variables we used here to estimate age at death agree with the arthroscopic observations of Noguchi et al. (41) who reported that, in prearthritic hip joints with normal radiological morphology, the first morphological changes of the acetabulum appear on the lip as small detaching tears, and on the outer edge of the acetabular fossa as small bony accretions such as osteophytic formations that grow near the fossa. This bone growth on the outer edge of the acetabular fossa can eventually occupy the entire fossa resulting in its total obliteration, with the collateral decrease of fibro-fatty, pulvinar tissue. In addition to this osteophytic formation (referred to as activity) on the outer edge of the acetabular fossa, we observed also a progressive change in the osteological texture (referred to as activity and porosities) of the fossa in which the modification of the smooth bone reveals the trabecular bone. The changes undergone by the acetabulum have a certain similarity to the changes of the auricular surface with increasing age, as described by Lovejoy et al. (18). In both, porosities, ostophytic formations and characteristics compatible with degenerative osteoarthritis are evident in both.

The applicability of variables such as those we describe here for estimating age at death depends on the adequacy of the collections that provide data to establish the relationship between the states of the variables and known age at death. When such data are not

TABLE 6—*Number of specimens with fit (f), less than specified amounts, tabulated within age classes, and over all specimens.*

Age	$f<1$	$f<2$	$f<3$	$f<4$	$f<5$	$f<10$	$f>10$	Not Estimated	Total
15–19	3	6	6	7	7	9	0	0	9
20–24	10	12	16	17	17	20	1	0	21
25–29	1	1	6	11	15	23	2	1	26
30–34	2	7	14	21	23	25	0	0	25
35–39	0	3	6	8	18	24	1	1	26
40–44	1	3	5	9	9	18	3	0	21
45–49	1	3	10	13	14	18	1	0	19
50–54	1	2	7	9	11	14	4	0	18
55–59	0	0	2	4	8	15	5	1	21
60–64	1	1	1	3	4	9	4	0	13
65–69	0	0	1	2	6	12	1	0	13
70–74	0	2	4	4	5	11	1	0	12
75–79	0	0	0	0	1	7	3	1	11
80–84	0	3	3	3	3	4	1	0	5
85–89	1	1	1	1	1	1	0	0	1
90–94	0	0	0	0	0	0	0	0	0
95–99	1	1	1	1	1	1	0	0	1
Total	22	45	83	113	143	198	27	4	242

Fit is the expected value of absolute difference between the known age and the nearest age in any age class, except the one in which the known age falls.

sufficient, it will not be possible to estimate age at death for some individuals. In the results reported here, scores from four of 242 individuals did not result in an estimate of age at death because there were insufficient data.

Using the seven variables based on the acetabulum and the computational methods we describe produces encouragingly accurate estimates in the form of probability distributions over 5-year age classes. The most immediate and conspicuous indication of the potential utility of these variables to estimate age at death is revealed by comparing known age at death with the estimated probability distribution of age classes, using measures of fit and comparing known age at death with expected values. All ages were estimated with good levels of accuracy, indicating that observations from the acetabular area may be useful to estimate age at death in adult individuals of any age, even those who died at over 40 years of age. This accuracy for older ages is largely explained by the longer maturation and aging time course of the anatomical features of the acetabulum used to estimate age at death.

The estimates we present here are seen to be more accurate than those of most previous workers because the estimating probability distributions have lower variances, estimating intervals have shorter time spans, and estimates are closer to the known ages at death. Higher variances reflect a trade-off that increases the chance that known age at death will fall inside the distribution but decreases the precision of the estimate. In the results we present here, based on observation of the acetabulum, the estimating distribution tends to be both narrow and centred near known age at death, with age at death for adolescents, middle aged adults, and elderly all estimated with similar levels of accuracy.

Only a few authors report comparable levels of accuracy. Schmitt (30) and Schmitt et al. (35) used observations on the auricular surface and the pubic symphysis. However, these authors encountered difficulties with estimates of age at death for specimens older than 60 years, and so lumped into a single age class all specimens who died at age 60 years or older, obscuring inaccuracies there. These difficulties are probably because of the unreliability of the auricular surface and the pubis symphysis as estimators of age at death in adults over 40 years old. Because we use the probability distributions themselves and several operationally defined and quantitative descriptions of estimated age at death derived from them to evaluate accuracy, it is difficult to make a more specific comparison with the more subjective evaluations employed by some authors. Wittwer-Backofen et al. (11) report accurate estimates of age for living individuals, based on microscopic measurements of extracted teeth, but such data are rarely available to archaeologists and palaeontologists.

Conclusion

From the previous results of age analysis on the acetabular area (27) based on a small Spanish and French sample and the results reported here based on a Portuguese sample we can conclude that the acetabulum seems to be an effective age predictor. The seven age indicators described in the present work, based on measures of the acetabulum, can be useful to estimate age at death of unknown specimens of any age with fused acetabulum with same accuracy (89% in 10-year intervals or 67% in 5-year interval), including individuals who fall at the far end of the aging distribution. In addition, the acetabulum is an especially convenient structure to observe in ancient and forensic remains because, as part of the central area of the os coxa, it is one of the best-preserved elements of the skeleton (42). For this reason it seems useful and necessary to increase the research on the acetabulum as an age indicator in order to understand better the behavior of this anatomical structure during the aging process in the different populations.

Acknowledgments

We acknowledge the advice and assistance of the staff of the Knowledge Center of the University of Michigan and of Virginia Hutton in the preparation of the graphics. We thank Lluis Lloveras, Victor Matos, and Cristina Santos for collaborating in testing observational consistency of the variables.

References

1. Buckberry JL, Chamberlain AT. Age estimation from the auricular surface of the ilium: a revised method. Am J Phys Anthropol 2002;119:231–9.
2. Mays S. The archaeology of human bones. London: Routledge; 1998.
3. Bocquet-Appel JP, Masset C. Farewell to the paleodemography. J Hum Evol 1982;12:321–33.
4. Boldsen JL. Two methods for reconstruction of the empirical mortality profile. Hum Evol 1988;3:335–42.
5. Konigsberg LW, Frankenberg SR. Estimation of age structure in anthropological demography. Am J Phys Anthropol 1992;89:235–56.
6. Lovejoy CO, Meindl RS, Mensforth RP, Barton TJ. Multifactorial age determination of skeletal age at death: a method and blind tests of its accuracy. Am J Phys Anthropol 1985;68:1–14.
7. Krogman WM, Işcan MY. The human skeleton in forensic medicine. 1st ed. Springfield, IL: Charles C. Thomas; 1986:103–88.
8. Işcan MY. Age markers in human skeleton. Springfield, IL: Charles C. Thomas; 1989.
9. Stout SD. The application of histological techniques for age at death determination. In: Reichs KJ, editor Forensic osteology. Advances in the identification of human remains. Springfield, IL: Charles C. Thomas; 1997:237–52.
10. Boldsen JL, Milner GR, Konigsberg LW, Wood JW. Transition analysis: a new method for estimating age from skeletons. In: Hoppa RD, Vaupel JW, editors. Paleodemography. Age distributions from skeletal samples. Cambridge: Cambridge University Press; 2002:73–106.
11. Wittwer-Backofen U, Gampe J, Vaulpel JW. Tooth cementum annulation for age estimation: results from a large known-age validation study. Am J Phys Anthropol 2004;123:119–29.
12. Todd TW. Age changes in the pubic bone: the male white pubis. Am J Phys Anthropol 1921;3:285–339.
13. Brooks ST. Skeletal age at death. The reliability of cranial and pubic age indicators. Am J Phys Anthropol 1955;13:567–59.
14. Brooks S, Suchey JM. Skeletal age determination based on the os pubis: a comparison of the Ascádi-Nemeskeri and Suchey-Brooks methods. Hum Evol 1990;5(3):227–38.
15. Lovejoy CO, Meindl RS, Tague RG, Latimer B. The senescent biology of the hominoid pelvis. Riv Antropol 1995;73:31–49.
16. Schmitt A, Broqua C. Approche probabilistique pour estimer l'âge au dêcès a partir de la surface auricülare de l'ilium. Bull Mém Soc Anthropol París 2000;5:293–300.
17. Scheuer L, Black S. Developmental juvenile osteology. London: Academic Press; 2000:368–71.
18. Lovejoy CO, Meindl RS, Pryzbeck TR, Mensforth RP. Chronological metamorphosis of the auricular surface of the ilium: a new method for the determination of adult skeletal age at death. Am J Phys Anthropol 1985;68:15–28.
19. Bedford ME, Russel KF, Lovejoy CO, Meindl RS, Simpson SW, Stuart-Macadam PL. Test of the multifactorial aging method using skeletons with known ages-at-death from the Grant Collection. Am J Phys Anthropol 1993;91:287–97.
20. Murray KA, Murray T. A test of the auricular surface aging technique. J Forensic Sci 1991;6(4):1162–9.
21. Saunders SR, Fitzgerald C, Rogers T, Dudar C, Mckillop H. A test of several methods of skeletal age estimation using a documented archaeological sample. Canadian Soc Foren Sci 1992;25:97–118.
22. Santos AL. How old is this pelvis? A comparison of age at death estimation using the auricular surface of the ilium and os pubis. In: Pwiti G, Soper RA, editors. Aspects of African archaeology. Proceedings of the 10th Congress of the Pan African Association for Prehistory and Related Studies; 1995 Jun 18–23; Harare. Zimbabwe: Print Holdings; 1996: 29–36.

23. Rissech C, Malgosa A. Longitud del isquion desde el nacimiento hasta la vejez: diagnóstico de edad y sexo. In: Varela T, editor. Investigaciones en Biodiversidad Humana. Santiago de Compostela (Spain): Universidad de Santiago de Compostela; 2000:350–7.
24. Rissech C. Anàlisi del creixement del coxal a partir de material ossi i les seves aplicacions en la Medicina Forense i l'Antropologia, Ph.D. dissertation, Universitat Autònoma de Barcelona, Barcelona, 2001;63–72.
25. Rissech C, Sañudo JR, Malgosa A. Acetabular point: a morphological and ontogenetic study. J Anatomy 2001;198:743–8.
26. Rougé-Maillart C. Estimation de l'âge à partir de la partie postérieure du bassin: étude comparée de la surface auriculaire et du cotyle, diplôme d'étude approfondie d', Anthropologie dissertation, Université de Toulouse le Mirail, Toulouse, 2000.
27. Rougé-Maillart CL, Telmon N, Rissech C, Malgosa A, Rougé D. The determination of male adult age by central and posterior coxal analysis. A preliminary study. J Forensic Sci 2004;49:1–7.
28. Rocha MA. Les collections ostéologiques humaines identifiées du Musseé Anthropologique de l' Université de Coimbra. Antropologia Portuguesa 1995;13:17–38.
29. Cunha E. Osteoarthritis as an indicator of demographic structure of past populations: the example of a Portuguese medieval sample. In: Perez-Perez A, editor. Salud, enfermedad y muerte en el pasado. Consecuencias biologicas del estrés y la patologí. Barcelona: Fundación Uriach; 1838, 1996:149–55.
30. Schmitt A. Variabilité de la sénescence du squelette humain. Réflexions sur les indicateurs de l'âge au décès: à la recherche d'un outil performant, Ph.D. dissertation, Universite de Bordeaux I, Bordeaux, 2001.
31. Kruskal WH, Wallis WA. Use of ranks in one-criterion variance analysis. J Am Stat Asso 1952;47:583–621.
32. Benzecri JP. L'analyse des données: T.2, l'analyse des correspondences. Paris: Dunod; 1973.
33. Siegel S. Nonparametric statistics for the behavioural sciences. New York: McGraw-Hill; 1956.
34. Lucy D, Aykroyd RG, Pollard AM, Solheim T. A Bayesian approach to adult human age estimation from dental observations by Johanson's age changes. J Forensic Sci 1996;41:189–94.
35. Schmitt A, Murail P, Cunha E, Rougé D. Variability of the pattern of ageing on the human skeleton: evidence from bone indicators and implications on age at death estimation. J Forensic Sci 2002;47:348–476.
36. Gowland RL, Chamberlain AT. A Bayesian approach to ageing perinatal skeletal material from archaeological sites: implications for the evidence for infanticide in Roman-Britain. J Archaeol Sci 2002;29:677–85.
37. Aykroyd RG, Lucy D, Pollard AM, Roberts CA. Nasty, brutish, but not necessarily short: a reconsideration of the statistical method used to calculate age at death from adult human skeletal and dental age indicators. Am Antiq 1999;64:55–70.
38. Hedges REM, Millard A. Measurements and relationships of diagenetic alteration of bone from three archaeological sites. J Archaeol Sci 1995a; 22:201–9.
39. Hedges REM, Millard AR. Bones and groundwater: towards the modelling of diagenetic processes. J Archaeol Sci 1995b;22:155–164.
40. Lazennec JY, Laudet CG, Guérin-Surville H, Roy-camille R, Saillant G. Dynamic anatomy of the acetabulum: an experimental approach and surgical implications. Surg Radiol Anat 1997;19:23–30.
41. Noguchi Y, Miura H, Takasugi S, Iwamoto Y. Cartilage and labrum degeneration in the dysplastic hip generally originates in the anterosuperior weight-bearing area: an arthroscopic observation. J Arthrosco Rela Surg 1999;15(5):496–506.
42. Rissech C, Malgosa A. Sex prediction by discriminant function with central portion measures of innominate bones. Homo 1997;48(1):22–32.

Additional information and reprint requests:
Carme Rissech, Ph.D.
Unitat d'Antropologia
Departament de Biologia Animal, Vegetal i Ecologia
Facultat de Ciències
Universitat Autònoma de Barcelona
08193 Bellaterra
Spain
E-mail: rissechc@ci.uc.pt